# POLYDOPAMINE COATING EFFECTIVELY PREVENTS EARLY-STAGE CORROSION OF PURE MAGNESIUM IN TISSUE CULTURE MEDIUM

**Kotomi Kitada[1,2], Sayuki Yoshitomi[1,2], Minori Sugiyama[1,2], Taiki Morishige[1], Sachiro Kakinoki[1,2,*]**

[1] Faculty of Chemistry, Materials, Bioengineering, Kansai University, 3-3-35 Yamate, Suita, Osaka 564-8680, Japan
[2] Kansai University Medical Polymer Research Center (KUMP-RC), Kansai University, 3-3-35 Yamate, Suita, Osaka 564-8680, Japan
*e-mail: sachiro@kansai-u.ac.jp

## Abstract

*Pure magnesium, free from toxic elements, has been identified as a promising candidate for bioabsorbable orthopaedic devices. However, its rapid corrosion in physiological environments presents a significant challenge for practical applications. Chemical coatings, such as polydopamine (PDA), offer a potential solution to improve the corrosion resistance of pure magnesium. Nevertheless, the reaction conditions must be meticulously optimized, particularly in the presence of salts, as magnesium is highly sensitive to environmental factors. In this study, a PDA coating, widely investigated for improving the corrosion resistance of magnesium alloys, was applied to pure magnesium, avoiding the conventional Tris-HCl buffer. Instead, a 0.01 mol/L NaOH aqueous solution was used successfully to coat PDA layer on the surface of pure magnesium. The corrosion behaviour of PDA-coated magnesium was evaluated using electrochemical measurements and magnesium ion elution profiles in a tissue culture medium containing 5 vol% of fetal bovine serum at 37ºC. The results demonstrated that the PDA coating effectively mitigated early-stage corrosion of the pure magnesium substrate. This method provides a straightforward approach to enhancing the corrosion resistance of pure magnesium, and the PDA layer can also function as an intermediate platform for further biofunctional surface modifications, potentially expanding its applications in biomedical fields.*

***Keywords:*** *pure magnesium, polydopamine, coating, corrosion resistance, tissue culture medium*

## Introduction

Metallic materials, such as titanium (Ti) alloys, stainless steels, and Co-Cr alloys, which form stable and biocompatible passive layers, have been widely used for bone fixation devices [1,2]. Ti alloys are widely employed as a substrate for these devices due to their high corrosion resistance and osseointegration properties. Although the elastic modulus of Ti alloys (≈100 GPa) is closer to cortical bone (10-30 GPa) compared to SUS316L (≈200 GPa), the placement of Ti alloy devices increases stress shielding, leading to delayed bone regeneration and atrophy [3]. Additionally, wear debris and metal ions released from metallic devices can induce chronic inflammation and allergic reactions [4]. Non-biodegradable metallic devices also require surgical removal, which is highly invasive and prolongs the recovery period [5]. Therefore, there is a need to develop bone fixation device substrates that offer both an elastic modulus similar to bone tissue and biodegradability within the body.

Recently, magnesium (Mg), a biodegradable metal, has gained attention as a potential substrate for bone fixation devices. Mg is an essential element for the body, which contributes to its excellent biocompatibility. The density (1.74 g/cm³) and Young's modulus (40-45 GPa) of Mg are similar to those of bone (density: 1.75 g/cm³, Young's modulus: 10-27 GPa), suggesting its potential to avoid stress shielding [6-8]. Furthermore, $Mg^{2+}$ ions have been reported to promote bone tissue growth by activating osteoblasts [9]. However, pure Mg undergoes rapid corrosion in physiological environments, generating hydrogen gas that forms voids between surrounding tissues when implanted as a device, leading to tissue layer separation and necrosis [10-12]. Local alkalization around pure Mg also occurs due to the formation of $Mg(OH)_2$ during corrosion, which leads to severe haemolysis of red blood cells [13]. Consequently, rapid corrosion of pure Mg devices results in the loss of their mechanical properties before the bone defect is fully repaired [14]. Currently, Mg alloys are preferred as substrates of implantable devices due to their slower corrosion rate compared to pure Mg. The clinically available Mg alloy, MgYREZr, has been used in Europe as the bone fixation screw MAGNEZIX® (Syntelix AG, Germany) [4]. However, the toxicity of rare earth metals, such as yttrium, used in Mg alloys remains a significant concern [15].

To address corrosion issues, surface modification of pure Mg and Mg alloys has been widely investigated. Surface modification is a promising strategy not only to reduce the corrosion rate but also to improve the biocompatibility of Mg substrates. Various approaches such as anodic oxidation [16], micro-arc oxidation [17], electrodeposition [18], and sol-gel methods [19], have been applied to delay the early-stage corrosion of Mg alloys. Although these methods effectively enhance corrosion resistance, they do not provide osteoconductivity to Mg alloys, which should also be considered for orthopaedic applications.

Surface modification using hydroxyapatite (HAp) has been extensively studied to suppress corrosion and improve the osteoconductivity of Mg alloys, as HAp is a crucial inorganic component of cortical bone that promotes osteoblast proliferation [20]. Hiromoto et al. reported that HAp coatings on pure Mg and Mg alloys such as AZ31, AZ61, and AZ91 using a calcium-chelate compound, reduce corrosion current densities by a factor of $10^3$-$10^4$ times compared to the as-polished samples in 3.5 wt% NaCl solution [21]. However, HAp coatings are brittle and prone to collapse due to hydrogen gas generation during corrosion [22,23].

***[Engineering of Biomaterials 172 (2024) 05]***

***doi:10.34821/eng.biomat.172.2024.05***

***Submitted: 2024-07-04, Accepted: 2024-07-25, Published: 2024-07-29***

**TABLE 1. Chemical composition (wt%) of pure Mg plates.**

| Element | Al | Zn | Mn | Si | Fe | Cu | Ni | Mg |
|---|---|---|---|---|---|---|---|---|
| wt% | 0.0024 | 0.0076 | 0.0017 | 0.0068 | 0.0050 | <0.0005 | <0.0005 | Bal. |

Polydopamine (PDA), inspired by mussel adhesion, offers several advantages for surface modification of pure Mg and Mg alloys, including a simple preparation process, low toxicity, high reactivity, and easy functionalization via catechol groups. For example, Zhou et al. demonstrated that PDA coating significantly improved the corrosion resistance of the AZ31 alloy [24]. Previous studies have commonly employed a dopamine (DA) solution prepared with a Tris-HCl buffer solution at weak alkalinity (pH = 8.5) for PDA coating on Mg alloys. However, this method is not suitable for pure Mg, as it leads to immediate corrosion in the solution containing chloride ions [25].

In this study, a suitable solution for PDA coating on pure Mg was investigated using sodium hydroxide aqueous solutions at different pH values. The PDA-coated pure Mg was characterized, and its corrosion resistance was evaluated through potentiodynamic polarization test and the elution behaviour of $Mg^{2+}$ ions in a tissue culture medium containing fetal bovine serum.

## Materials and Methods

### Materials

Pure Mg substrates cut into plate shape (5.0×5.0 mm or 10×10 mm, thickness: 1.0 mm) were generously provided by Japan Fine Steel Co., Ltd (Yamaguchi, Japan). The chemical composition of the pure Mg substrates is detailed in TABLE 1. Isopropyl alcohol, ethyl alcohol, sodium hydroxide, penicillin/streptomycin mixed solution, hydrochloric acid (1 mol/L), and magnesium nitrate hexahydrate were obtained from Nakalai Tesque Inc (Kyoto, Japan). Dopamine hydrochloride and N, N-dimethylformamide (DMF) were purchased from Tokyo Chemical Industry Co., Ltd. (Tokyo, Japan) and Watanabe Chemical Industries Co., Ltd. (Hiroshima, Japan), respectively. Conductive adhesive (Dotite D-500) and epoxy resin used for electrochemical corrosion tests were purchased from Fujikura Kasei Co., Ltd. (Tokyo, Japan) and IMT Co., Ltd. (Wakayama, Japan), respectively. Fetal bovine serum (FBS) for preparing tissue culture medium was purchased from ATLAS BIOLOGICALS (Colorado, United States). Xylidyl Blue-I for detecting $Mg^{2+}$ ions during corrosion tests was purchased from Metallogenics Co.,Ltd. (Chiba, Japan).

### Surface modifications

Before surface modification, the pure Mg plates were polished using a tabletop polishing machine (IM-P2: IMT Co., Ltd., Wakayama, Japan) with abrasive papers (Sankyo Rikagaku Co. Ltd., Saitama, Japan) up to 3000 with ultrapure water. Subsequently, the pure Mg plates were mirror-polished using alumina powder (0.3 μm) diluted in isopropyl alcohol. The mirror-polished pure Mg plates were sequentially sonicated in DMF and ethyl alcohol, and then dried in the oven at 50°C. The mirror-polished pure Mg plates were immersed in 1 mol/L sodium hydroxide (NaOH) aqueous solution at 75°C for 24 h for hydroxide passivation. The alkali-treated pure Mg plates were then cleaned with ultrapure water and dried again in the oven (50°C).

Alkali-treated pure Mg plates were immersed in 1.8 mL of 0.01, 0.05, and 0.1 mol/L NaOH aqueous solutions, respectively, and heated to 50°C. Then, 0.2 mL of 20 mmol/L dopamine (DA) aqueous solution was added to each, and the reaction proceeded under shaking at 50°C for 24 h [26]. The DA-treated pure Mg plates were washed with ultrapure water and dried in the oven (50°C).

### Surface characterization

The surface morphology of the pure Mg plates (10×10 mm, thickness: 1.0 mm) with or without treatments was observed using a 3D laser microscope (OLS40-SU, EVIDENT, Tokyo, Japan). The surface elemental composition of each pure Mg plate (size: 5.0×5.0 mm, thickness: 1.0 mm) was analysed by X-ray photoelectron spectroscopy (XPS) (ESCA-3400, Shimadzu Corporation, Kyoto, Japan) with an Mg Kα (1253.6 eV) X-ray source. The static contact angle of a sessile water drop on each pure Mg plate (10×10 mm, thickness: 1.0 mm) was measured using a contact angle meter (CA-XP; Kyowa Interface Science Co., Ltd., Saitama, Japan).

### Electrochemical corrosion tests in tissue culture medium

The pure Mg plates (10×10 mm, thickness: 1.0 mm) were connected to a copper wire using Dotite D-500 dissolved in toluene. The copper wire was insulated with a polytetrafluoroethylene tube. The pure Mg plates attached with the copper wire were embedded in epoxy resin. The resin-embedded pure Mg plates were mirror-polished and then treated with 1 mol/L sodium hydroxide and DA solutions with different concentrations, as described previously. Electrochemical corrosion tests were conducted in 150 mL of αMEM medium containing 5 vol% of FBS, supplemented with penicillin-streptomycin using an automatic polarization system (HSV-110: MEIDEN HOKUTO Co., Ltd., Tokyo, Japan). The pure Mg plate, Ag/AgCl electrode, and stainless steel served as the working electrode, reference electrode, and counter electrode respectively, with applying voltages of 1 V and –1 V.

Corrosion rates were calculated according to the ASTM standard G102-89 [27] using equation (1):

$$CR_{electrochemical}\ [\text{mm/year}] = 3.27 \times 10^{-3} \times EW \times \frac{i_{corr}}{\rho} \quad (1)$$

where $EW$ is the equivalent weight of magnesium (valence 2), $i_{corr}$ is the current density [μA/cm$^2$], and $\rho$ is the theoretical density of pure magnesium [g/cm$^3$] [28].

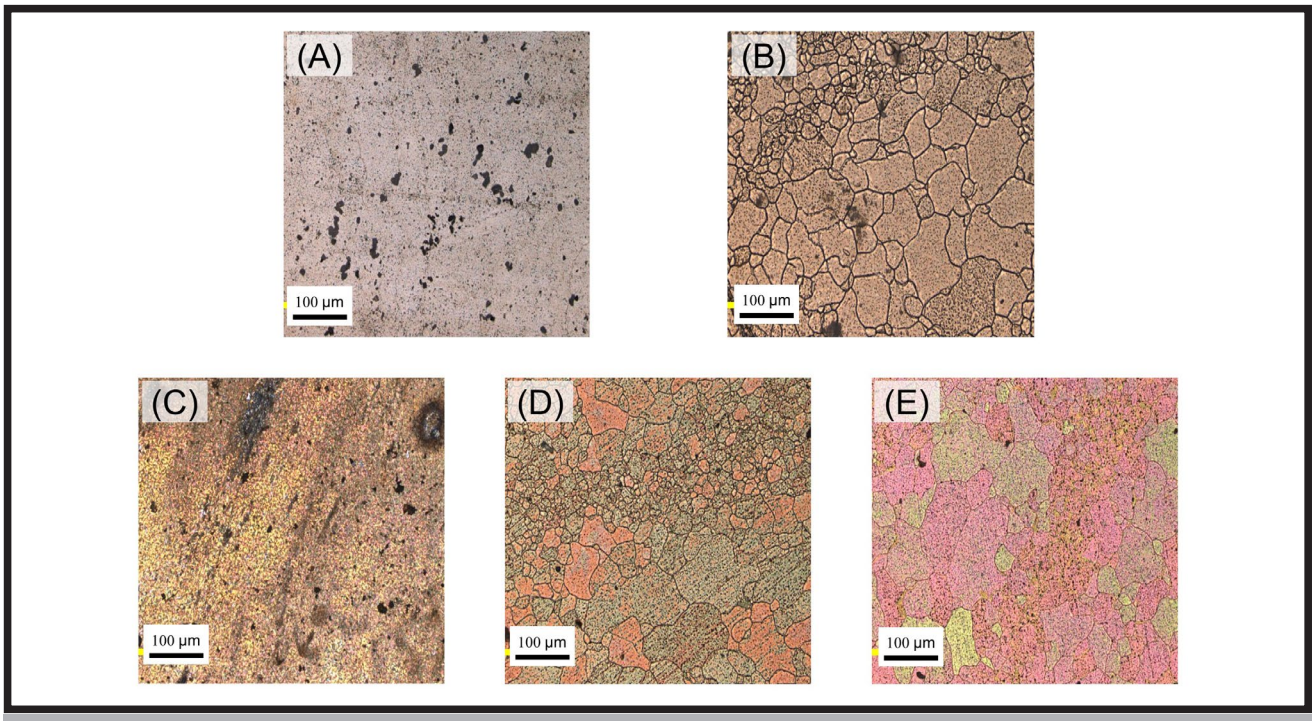


**FIG. 1. Morphological observation of Mg plate samples using 3D measurement laser microscope, (A) Bare Mg, (B) Mg-Alk, (C) Mg-Alk-DA0.01, (D) Mg-Alk-DA0.5 and (E) Mg-Alk-DA0.1.**

**$Mg^{2+}$ ions eluting tests in tissue culture medium**

The pure Mg plates (10×10 mm, thickness: 1.0 mm) with different treatments were embedded in the epoxy resin, exposing only one surface. The resin-embedded pure Mg plates were immersed in 5 mL of αMEM containing 5 vol% of FBS, supplemented with penicillin-streptomycin at 37°C. At each measurement points, the αMEM medium was collected and the pure Mg plates were immersed in 5 mL of fresh αMEM medium again. $Mg^{2+}$ ions eluted from the pure Mg plates were determined by comparing the collected αMEM with the fresh αMEM medium. The concentration of $Mg^{2+}$ ions in the medium was quantified using the Metal Assay Magnesium Detection LS Kit (Mettallogenics Co., Ltd., Chiba, Japan). Briefly, 30 μL of 1.0 mol/L hydrochloric acid was added to 1 mL of medium and mixed thoroughly with a vortex mixer. After standing at room temperature for 30 min, the mixture was centrifuged 5000 rpm at 4°C for 10 min, and 500 μL of the supernatant was collected as the assay sample. A 1.5 μL aliquot of the sample was placed into a 96-well plate, followed by the addition of 125 μL of Xylidyl Blue-I solution to each well. After the reaction for 5 min at room temperature, absorbance (λ = 660 nm) was measured using a plate reader (Spark 10M: TECAN Co., Ltd., Switzerland). The $Mg^{2+}$ concentration in αMEM was calculated using the following equation (2):

$$Mg^{2+}\ \text{concentration (mg/dl)} = \left(\frac{Abs_{sample} - Abs_{blank}}{Abs_{standard} - Abs_{blank}}\right) \times 2 \quad (2)$$

A standard solution (2 mg/dL) was included in the Metal Assay Magnesium Detection LS Kit, and a standard curve for calibrating the accurate concentration of $Mg^{2+}$ ions was prepared using αMEM containing magnesium nitrate at varying concentrations.

**Statistical analysis**

The results are expressed as the mean ± standard deviation. Statistical analysis was performed using one-way analysis of variance (ANOVA), followed by Tukey's post-hoc test for data comparison. Statistical significance was defined as $p < 0.05$.

## Results and Discussions

**Surface characterization**

The surface topology of pure Mg plates with different treatments was observed using a 3D laser microscope, as shown in FIG. 1. On the surface of Mg-Alk, crystal grain boundaries were visible due to etching under alkaline conditions. Similarly, crystal grain boundaries were observed on the surface of Mg-Alk-DA0.05 and Mg-Alk-DA0.1. However, a heterogeneous structure with no visible crystal grain boundaries was found on Mg-Alk-DA0.01.

The static contact angle of sessile water drops on pure Mg plates with different treatments is shown in FIG. 2. The water contact angle of the untreated pure Mg plate was 50.0°, which decreased to 32.0° on Mg-Alk. The alkali treatment led to the formation of magnesium hydroxide ($Mg(OH)_2$) passive film on the pure Mg plates, exposing hydrophilic hydroxyl groups on the outmost surface. Interestingly, the water contact angle on Mg-Alk-DA0.01 dropped to 6.4°. However, it increased to 57.6° and 32.6° on Mg-Alk-0.05 and Mg-Alk-1.0, respectively.

Binding and polymerization of DA is accompanied by the corrosion of pure Mg plates, which varies with the pH of the reaction solution. A strong alkaline condition (pH 8.5-10) is more favourable for the polymerization of DA, as PDA layer disassembles under strong alkaline conditions (pH>10) due to the deprotonation [29,30]. In this study, the pH values of DA solutions prepared with 0.01, 0.05 and 0.1 mol/L NaOH aqueous solution were 9.2, 12.0 and 12.5, respectively. Hence, it is suggested that the binding and polymerization of DA proceeded with suppressing the corrosion of pure Mg plates in DA solution prepared by 0.01 mol/L NaOH aqueous solution.

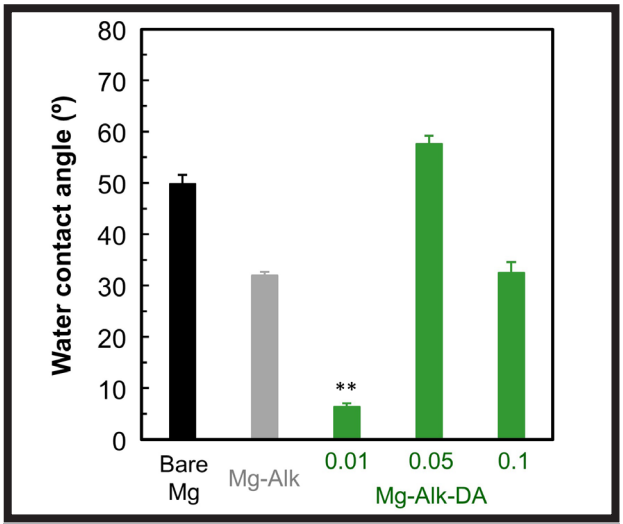


**FIG. 2. Water contact angle of the pure Mg plates with different treatments. **$p$<0.01 compared to the other pure Mg plates.**

**Chemical composition of the surface of pure Mg plates with different treatments**

The presence of a PDA layer on pure Mg plates was investigated by XPS, as shown in FIG. 3. The atomic compositions obtained from the XPS analyses are summarized in TABLE 2.

In the wide-scan spectrum, all pure Mg plates showed prominent peaks for C1s, O1s and Mg2p at approximately 285 eV, 532 eV and 51.0 eV, respectively. Additionally, pure Mg plates with PD treatment exhibited an N1s peak at around 400 eV. For the bare pure Mg plate, the presence of C1s is typically attributed to unavoidable hydrocarbon contamination, while the appearance of O1s and Mg2p assigned $Mg(OH)_2$ is due to rapid oxidation in the atmospheric environment. The appearance of both Mg2p with $MgCO_3$ (51.7 eV) and O1s with C=O (535 eV) on Mg-Alk suggests that $Mg(OH)_2$ reacted with $CO_2$ diffused from the environment during the alkaline treatment [31-33]. The N1s ratio was highest on the Mg-Alk-DA0.01 surface, while the Mg2s ratio representing the substrate was lowest. These results indicate that the pure Mg surface was successfully coated with the densest PDA layer in a 2.0 mmol/L DA solution prepared with 0.01 mmol/L NaOH at pH 9.2.

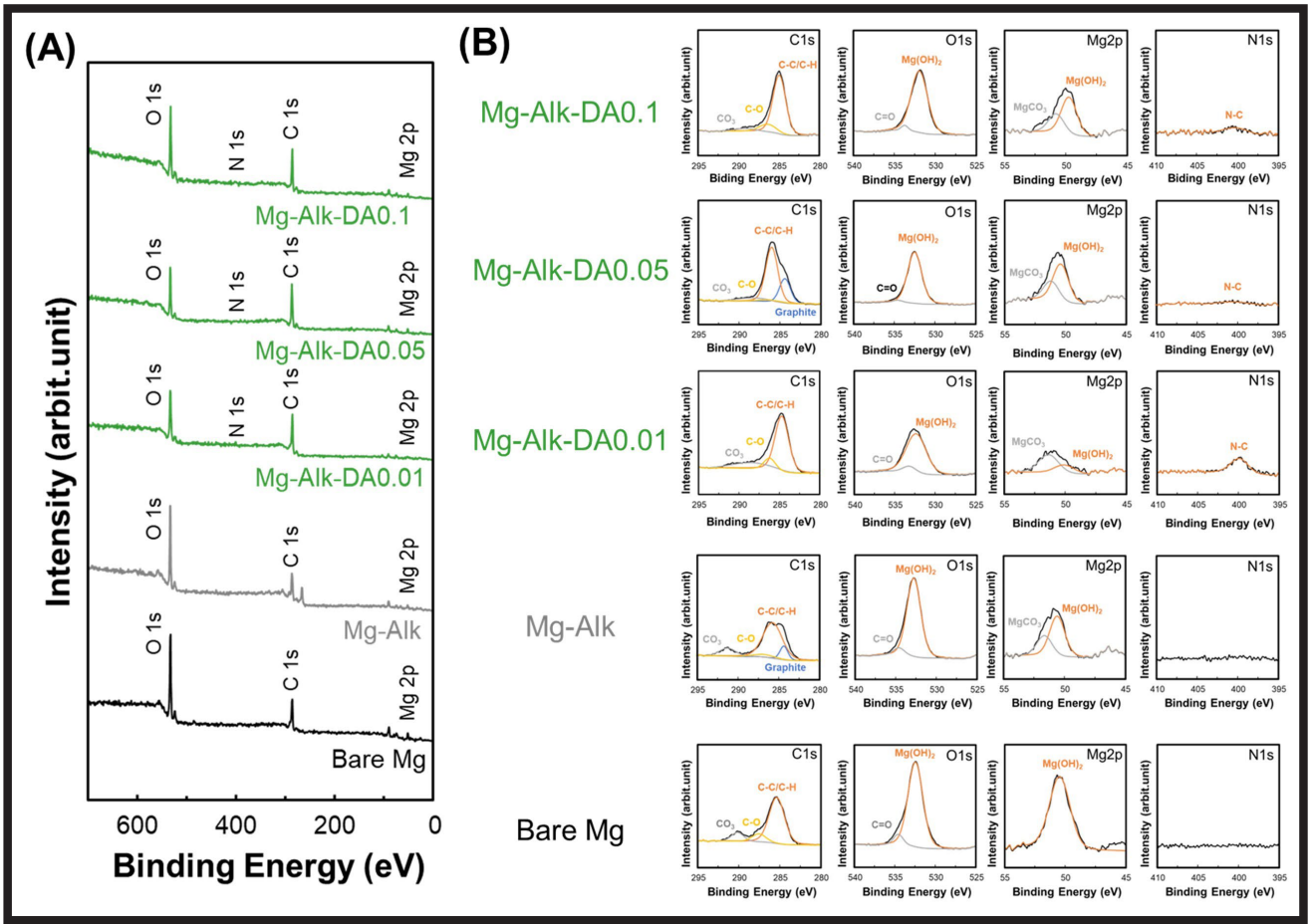


**FIG. 3. XPS analysis of pure Mg plates with different treatments, (A) wide scans and (B) narrow scans of C1s, O1s, Mg2p and N1s.**

**TABLE 2. Atomic composition of the surface of pure Mg plates with different treatments determined by XPS.**

| Samples | Element (Atomic %) | | | |
|---|---|---|---|---|
| | C1s | N1s | O1s | Mg2p |
| Bare Mg | 28.02 | - | 68.06 | 3.91 |
| Mg-Alk | 31.46 | - | 65.76 | 2.78 |
| Mg-Alk-DA0.01 | 42.47 | 3.33 | 52.41 | 1.79 |
| Mg-Alk-DA0.05 | 45.37 | 1.57 | 49.85 | 3.21 |
| Mg-Alk-DA0.1 | 35.63 | 1.42 | 60.00 | 2.95 |

**Electrochemical corrosion tests in tissue culture medium**

Potentiodynamic polarization curves and corrosion rate for Mg plates with different treatments in αMEM containing 5 vol% FBS are shown in FIG. 4. The bare pure Mg plate exhibited a typical polarization curve, indicating rapid corrosion in tissue culture medium (FIG. 4A) [34]. In this study, pure Mg plates containing 0.0017wt% Mn and 0.005wt% Fe (Fe/Mn = 2.94) were used. The corrosion rate is known to increase with higher Fe/Mn ratios, as Fe acts as a preferential initiation point for corrosion [35]. Thus, the corrosion of bare pure Mg plate was very rapid. The polarization curve for Mg-Alk was shifted to a more positive potential and the breakdown of passivity observed around -1.25 V in bare pure Mg plate disappeared, indicating an increase in corrosion resistance after alkaline passivation. For Mg-Alk-DA0.01, the anodic current density initially increased, followed by a sharp decrease around -1.25 V. The corrosion rate of the bare pure Mg plate was 23.5 $mmy^{-1}$, which decreased to 5.58 $mmy^{-1}$ after alkali passivation (FIG. 4B). The corrosion rate of Mg-Alk-DA0.01 further decreased to 2.73 $mmy^{-1}$, indicating that the PDA coating effectively enhances the corrosion resistance of pure Mg in tissue culture medium. This behaviour is likely due to the early-stage corrosion at cracks in the PDA layer, which are subsequently filled by a growing passive layer containing MgOH, $MgCO_3$ and magnesium phosphates as shown in FIG. 5 [36].

**$Mg^{2+}$ ions eluting test in tissue culture medium**

Changes in the appearance of pure Mg plates during the $Mg^{2+}$ eluting test in tissue culture medium are shown in FIG. 6A. The bare pure Mg plate exhibited corrosion pits within 1 h of immersion, accompanied by hydrogen gas generation, followed by significant corrosion and fragmentation after 48 h. While the drastic early-stage corrosion was prevented on Mg-Alk, pitting corrosion was observed after 24 h and gradually progressed. In contrast, no noticeable change in appearance was observed on Mg-Alk-DA0.01, even after 48 h. The elution profile of $Mg^{2+}$ ions from pure Mg plates in a tissue culture medium is shown in FIG. 6B. The amount of eluted $Mg^{2+}$ ions was slightly low, with no statistically significant difference in $Mg^{2+}$ ion elution observed among the different pure Mg plates over 48 h. While $Mg^{2+}$ concentration continued to increase in both bare pure Mg and Mg-Alk plates, it appeared to plateau in Mg-Alk-DA0.01 after 48 h. The elution of $Mg^{2+}$ ions from the bare pure Mg plate did not fully correspond to the observed changes in appearance. Virtanen reported that an amorphous calcium phosphate layer forms on the surface of pure Mg after immersion in a tissue culture medium [34]. This suggests that fragments generated by the rapid corrosion of bare pure Mg were immediately covered by a passive layer containing calcium phosphate, resulting in only a slight amount of $Mg^{2+}$ ion elution. As shown in FIG. 5, the elution of $Mg^{2+}$ ions from Mg-Alk-DA0.01 appeared to be suppressed after 24 h, likely due to cracks in the PDA layer being gradually filled by a passive layer.

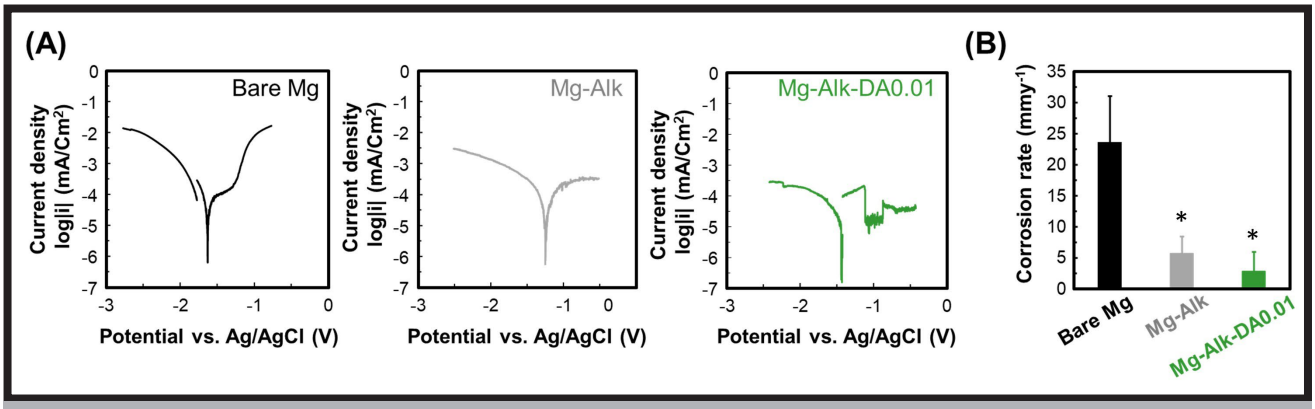


**FIG. 4. Electrochemical analysis of corrosion behavior of pure Mg plates with different treatments in tissue culture medium. (A) Potentiodyanmic polarization curves and (B) corrosion rate of Bare Mg, Mg-Alk and Mg-Alk-DA0.01. *$p$<0.05 compared to Bare Mg.**

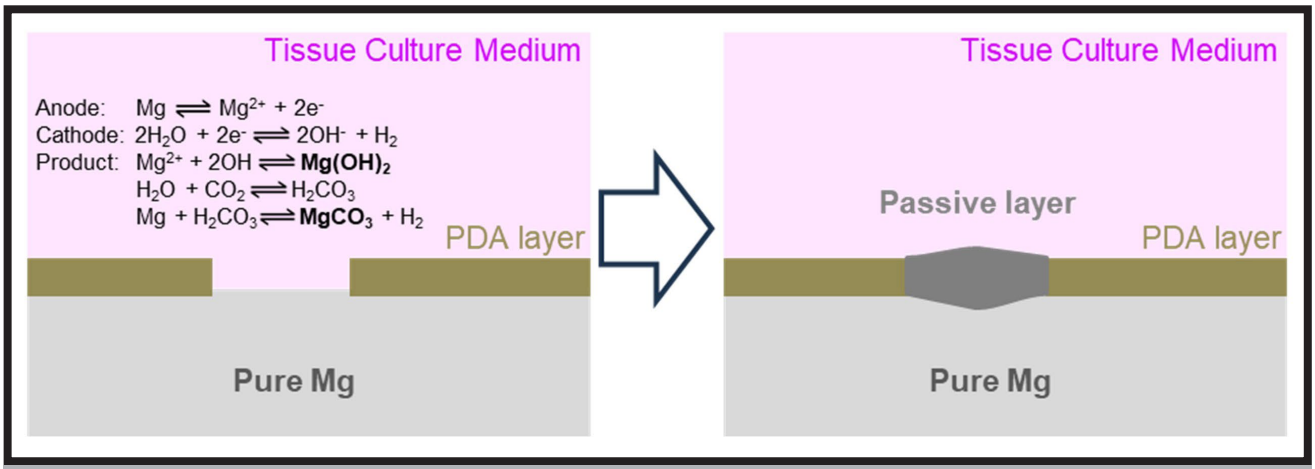


**FIG. 5. Proposed mechanism for the initial corrosion prevention by PDA layer on Mg-Alk-DA0.01 in tissue culture medium.**

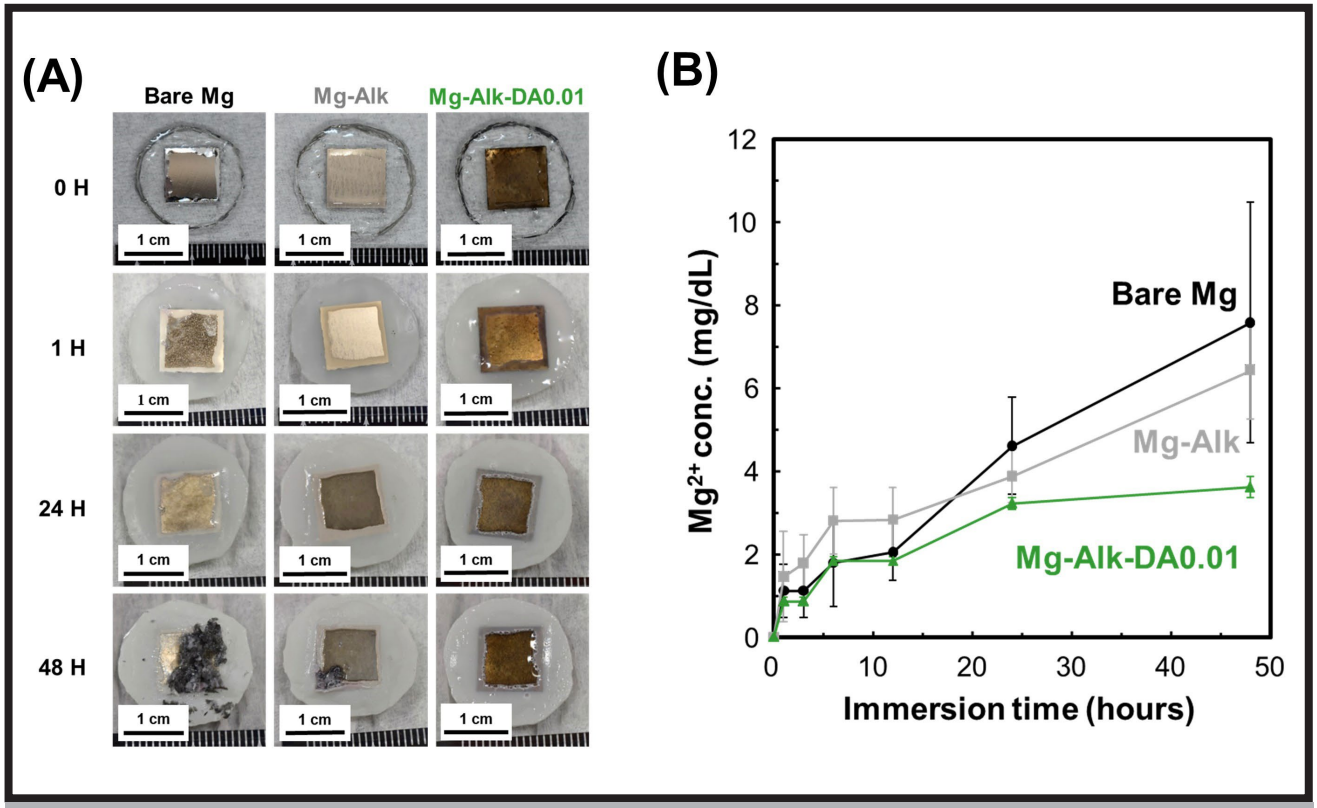


**FIG. 6. Corrosion behavior of pure Mg plates with different treatments in tissue culture medium. (A) Change of appearance and (B) elution profile of $Mg^{2+}$ ions.**

## Conclusions

The corrosion behaviour of pure Mg substrates is significantly influenced by various factors, including the composition and types of trace impurity elements, as well as the external environmental conditions. The use of polydopamine (PDA) modification for corrosion prevention in Mg alloys has been extensively studied. However, conventional PDA modification methods for Mg alloys are not suitable for pure Mg, which is more prone to rapid corrosion in alkaline buffer solutions containing chloride ions and polyhydric compounds. In this study, a PDA layer was successfully applied to the surface of pure Mg through an alkaline passivation process in 1.0 mol/L NaOH aqueous solution, followed by dopamine (DA) treatment in a 2.0 mmol/L DA solution prepared with 0.01 mmol/L NaOH at pH 9.2. Although the corrosion of pure Mg predominates over the polymeric reaction of DA in the conventional Tris-HCl buffer solution, it is drastically delayed, and the formation of the PDA layer on pure Mg progresses in a 1.0 mol/L NaOH aqueous solution without chloride ions or polyhydric compounds. The resulting PDA coating significantly improved the corrosion resistance of pure Mg in a tissue culture medium containing 5 vol% serum at 37°C, demonstrating its potential for biomedical applications. Further studies, including both *in vitro* and *in vivo* compatibility assessments, are required to demonstrate the feasibility of this PDA-coated pure Mg substrate for practical applications.

## Acknowledgements

*This research was partly supported by the Foundation of Chugoku Regional Innovation Research Center and the Takahashi Industrial and Economic Research Foundation. This research was partially funded by the Kansai University Fund for Supporting Young Scholars, 2021. The authors gratefully acknowledge Nao Ohtani, Mai Yoshikawa and Prof. Masato Ueda of Kansai University for their technical support. The authors wish to thank Japan Fine Steel Co., Ltd. (Yamaguchi, Japan) for generously providing pure magnesium plates.*

## References


[1] Nuevo-Ordóñez Y., Montes-Bayón M., Blanco-González E., Paz--Aparicio J., Raimundez J.D., Tejerina J.M., Peña M.A., Sanz-Medel A.: Titanium release in serum of patients with different bone fixation implants and its interaction with serum biomolecules at physiological levels. Anal Bioanal Chem 401 (2011) 2747–2754.

[2] Hiromoto S., Nozoe E., Hanada K., Yoshimura T., Shima K., Kibe T., Nakamura N., Doi K.: In vivo degradation and bone formation behaviors of hydroxyapatite-coated Mg alloys in rat femur. Materials Science & Engineering C 122 (2021) 111942.

[3] Biesiekierski A., Wang J., Gepreel M.A., Wen C.: A new look at biomedical Ti-based shape memory alloys. Acta Biomater. 8(5) (2012) 1661-1669.

[4] Sae-Mi K., Ji-Hoon J., Sung-Mi L., Min-Ho K., Hyoun-Ee K., Yuri E., Jong-Ho L., Jung-Woo L., Young-Hag K.: Hydroxyapatite-coated magnesium implants with improved in vitro and in vivo biocorrosion, biocompatibility, and bone response. Journal of Biomedical Materials Research A 102 (2013) 429-441.

[5] Seitz J.M., Lucas A., Kirschner M.: Magnesium-Based Compression Screws: A Novelty in the Clinical Use of Implants. The Minerals, Metals & Materials Society 68 (2016) 1177-1182.

[6] Chen Y., Xu Z., Smith C., Sankar J.: Recent advances on the development of magnesium alloys for biodegradable implants. Acta Biomaterialia 10 (2014) 4561-4573.

[7] Li N., Zheng Y.: Novel Magnesium Alloys Developed for Biomedical Application: A Review. Journal of Materials Science & Technology 29 (2013) 489-502.

[8] Kaabi Falahieh Asl S., Nemeth S., Tan M.J.: Novel biodegradable calcium phosphate/polymer composite coating with adjustable mechanical properties formed by hydrothermal process for corrosion protection of magnesium substrate. Journal of Biomedical Materials Research Part B: Applied Biomaterials 104 (2016) 1643-1657.

[9] Kim K.J., Choi S., Sang Cho Y., Yang S.J., Cho Y.S., Kim K.K.: Magnesium ions enhance infiltration of osteoblasts in scaffolds via increasing cell motility. Journal of Materials Science: Materials in Medicine 28 (2017) 96-104.

[10] Song G.: Control of biodegradation of biocompatible magnesium alloys. Corrosion Science 49 (2007) 1696-1701.

[11] Li L.Y., Cui L.Y., Zeng R.C., Li S.Q., Chen X.B., Zheng Y., Kannan M.B.: Advances in functionalized polymer coatings on biodegradable magnesium alloys - A review. Acta Biomaterialia 79 (2018) 23-36.

[12] Ren Y., Babaie E., Bhaduri S.B.: Nanostructured amorphous magnesium phosphate/poly (lactic acid) composite coating for enhanced corrosion resistance and bioactivity of biodegradable AZ31 magnesium alloy. Progress in Organic Coatings 118 (2018) 1-8.

[13] Zhen Z., Liu X., Huang T., Xi T., Zheng Y.: Hemolysis and cytotoxicity mechanisms of biodegradable magnesium and its alloys. Materials Science and Engineering C 46 (2015) 202-206.

[14] Wong H.M., Yeung K.W.K., Lam K.O., Tam V., Chu P.K., Luk K.D.K.: Cheung K.M.C., A biodegradable polymer-based coating to control the performance of magnesium alloy orthopaedic implants. Biomaterials 31 (2010) 2084-2096.

[15] Liu J., Liu B., Min S., Yin B., Peng B., Yu Z., Wang C., Ma X., Wen P., Tian Y., Zheng Y.: Biodegradable magnesium alloy WE43 porous scaffolds fabricated by laser powder bed fusion for orthopedic applications: Process optimization, in vitro and in vivo investigation. Bioactive Materials 16 (2022) 301-319.

[16] Lu X., Feng X., Zuo Y., Zhang P., Zhang C.: Improvement of protection performance of Mg-rich epoxy coating on AZ91D magnesium alloy by DC anodic oxidation. Progress in Organic Coatings 104 (2017) 188-198.

[17] Narayanan T.S.N.S., Park I.S., Lee M.H.: Strategies to improve the corrosion resistance of microarc oxidation (MAO) coated magnesium alloys for degradable implants: Prospects and challenges. Progress in Materials Science 60 (2014) 1-71.

[18] Zheng T., Hu Y., Pan F., Zhang Y., Tang A.: abrication of corrosion-resistant superhydrophobic coating on magnesium alloy by one-step electrodeposition method. Journal of Magnesium and Alloys 7 (2019) 193-202.

[19] Galio A.F., Lamaka S.V., Zheludkevich M.L., Dick L.F.P., Müller I.L., Ferreira M.G.S.: Inhibitor-doped sol–gel coatings for corrosion protection of magnesium alloy AZ31. Surface and Coatings Technology 204 (2010) 1479-1486.

[20] Lee J.Y., Han G., Kim Y.C., Byun J.Y., Jan J.I., Seok H.K., Yang S.J.: Effects of impurities on the biodegradation behavior of pure magnesium. Metals and Materials International 15 (2009) 955-961.

[21] Hiromoto S., Yamamoto A.: High corrosion resistance of magnesium coated with hydroxyapatite directly synthesized in an aqueous solution. Electrochimica Acta 54 (2009) 7085-7093.

[22] Song Y., Zhang S., Li J., Zhao C., Zhang X.: Electrodeposition of Ca–P coatings on biodegradable Mg alloy: In vitro biomineralization behavior. Acta Biomaterialia 6 (2010) 1736-1742.

[23] Ji X.J., Gao L., Liu J.C., Wang J., Cheng Q., Li J.P., Li S.Q., Zhi K.Q., Zeng R.C., Wang Z.L.: Corrosion resistance and antibacterial properties of hydroxyapatite coating induced by gentamicin--loaded polymeric multilayers on magnesium alloys. Colloids and Surfaces B: Biointerfaces 179 (2019) 429-436.

[24] Zhou Z., Zheng B., Lang H., Qin A., Ou J.: Corrosion resistance and biocompatibility of polydopamine/hyaluronic acid composite coating on AZ31 magnesium alloy. Surfaces and Interfaces 20 (2020) 100560.

[25] Cheng W., Zeng X., Chen H., Li Z., Zeng W., Mei L., Zhao Y.: Versatile Polydopamine Platforms: Synthesis and Promising Applications for Surface Modification and Advanced Nanomedicine. ACS Nano 13 (2019) 8537-8565.

[26] Ju K.Y., Lee Y., Lee S., Park S.B., Lee J.K.: Bioinspired Polymerization of Dopamine to Generate Melanin-Like Nanoparticles Having an Excellent Free-Radical-Scavenging Property. Biomacromolecules 12 (2011) 625-632.

[27] ASTM G102-89(2015), Standard Practice for Calculation of Corrosion Rates and Related Information from Electrochemical Measurements. ASTM International, West Conshohocken, PA, 2015.

[28] Putra N.E., Leeflang M.A., Minneboo M., Taheri P., Fratila--Apachitei L.E., Mol J.M.C., Zhou J., Zadpoor A.A.: Extrusion--based 3D printed biodegradable porous iron. Acta Biomaterialia 121 (2021) 741-756.

[29] Barclay T.G., Hegab H.M., Clarke S.R., Ginic-Markovic M.: Versatile Surface Modification Using Polydopamine and Related Polycatecholamines: Chemistry, Structure, and Applications. Advance Materials Interfacfes 4 (2017) 1601192.

[30] Lee H.A., Ma Y., Zhou F., Hong S., Lee H.: Material-Independent Surface Chemistry beyond Polydopamine Coating. Accounts of Chemical Research 52 (2019) 704-713.

[31] Moseley P.T., Tapping G., Rivière J.C.: The oxidation of dilute iron-silicon alloys ([Si] ≤ 1%) in carbon dioxide. Corrosion Science 22 (1982) 69-86.

[32] Yao H.B., Le Y., Wee A.T.S.: Passivity behavior of melt-spun Mg–Y Alloys. Electrochimica Acta 48 (2003) 4197-4204.

[33] Jönsson M., Persson D., Thierry D.: Corrosion product formation during NaCl induced atmospheric corrosion of magnesium alloy AZ91D. Corrosion Science 49 (2007) 1540-1558.

[34] Wagener V., Virtanen S.: Protective layer formation on magnesium in cell culture medium. Materials Science and Engineering: C 63 (2016) 341-351.

[35] Matsubara H., Ichige Y., Fujita K., Nishiyama H., Hodouchi K.: Effect of impurity Fe on corrosion behavior of AM50 and AM60 magnesium alloys. Corrosion Science 66 (2013) 203-210.

[36] Mei D., Lamaka S.V., Lu Z., Zheludkevich M.L.: Selecting medium for corrosion testing of bioabsorbable magnesium and other metals – A critical review. Corrosion Science 171 (2020) 108722.